

<https://helda.helsinki.fi>

The Finnish National Seismic Network : Toward Fully pö Automated Analysis of Low Magnitude Seismic E

Veikkolainen, Toni

2021-04-29

Veikkolainen , T , Kortström , J , Vuorinen , T , Salmenperä , I E , Luhta , T , Mäntyniemi , P , Hillers , G & Tiira , T 2021 , ' The Finnish National Seismic Network : Toward Fully pö Automated Analysis of Low Magnitude Seismic Events ' , Seismologica vol. 92 , no. 3 , pp. 1581-1591 . <https://doi.org/10.1785/0220200352>

<http://hdl.handle.net/10138/340878>
<https://doi.org/10.1785/0220200352>

acceptedVersion

Downloaded from Helda, University of Helsinki institutional repository.

This is an electronic reprint of the original article.

This reprint may differ from the original in pagination and typographic detail.

Please cite the original version.



1 **The Finnish National Seismic Network: Towards Fully** 2 **Automated Analysis of Low-Magnitude Seismic Events**

3

4 Toni Veikkolainen*, Jari Kortström, Tommi Vuorinen, Ilmo Salmenperä, Tuija Luhta, Päivi
5 Mäntyniemi, Gregor Hillers, and Timo Tiira

6

7 Institute of Seismology, University of Helsinki, P.O. Box 68, 00014 University of Helsinki,
8 Finland

9 * corresponding author, email: toni.veikkolainen@helsinki.fi

10

11 Most appropriate Flinn-Engdahl region: 721 Finland

12 Classification terms: 1 Seismic Arrays, Networks and Instrumentation, 12.300 Lithosphere, 14
13 Seismicity, 16.700 Stable Continental

14

15 **Declaration of Competing Interests**

16

17 The authors acknowledge there are no conflicts of interest recorded.

18

19 **Abstract**

20

21 We present an overview of the seismic networks, products, and services in Finland, northern
22 Europe, and the challenges and opportunities associated with the unique combination of

23 prevailing crystalline bedrock, low natural intraplate seismic background activity, and a high
24 level of anthropogenic seismicity. We introduce national and local seismic networks, explain the
25 databases, analysis tools, and data management concepts, outline the Finnish macroseismic
26 service, and showcase data from the 2017 M3.3 Liminka earthquake in Ostrobothnia, Finland.

27

28 **Introduction**

29

30 The first serious intent to join the international activities of the new discipline of seismology was
31 proposed at the meeting of the Geographical Society of Finland on 24 May 1902 (Simojoki
32 1978). It was only after Finland gained its independence in 1917, however, that these plans were
33 successfully implemented. A seismic station equipped with Mainka seismographs was in
34 operation in the Finnish capital Helsinki from 1924 to the early 1960s. This became the main
35 Finnish contribution to global seismology in the early instrumental era. The International
36 Geophysical Year of 1957-1958 gave an incentive to the deployment of various geophysical
37 instruments in the country, including seismographs (Pirhonen 1996), which facilitated short-
38 period seismology and the monitoring of local seismic events. The Comprehensive Nuclear Test
39 Ban Treaty Organization (CTBTO) was a major reason behind the establishment of the Institute
40 of Seismology, University of Helsinki (ISUH) in 1961 (Luosto and Hyvönen, 2001). The FINES
41 seismic array in Sysmä, Central Finland, serves today as one of the 50 global primary monitoring
42 stations of the CTBTO (Coyne et al., 2012). The modern network has improved seismic event
43 detection capabilities on the Finnish territory and adjacent areas, and frequent local network
44 densifications continue to challenge the associated data processing and management facilities.

45

46 **Current Seismic Networks in Finland**

47

48 In 2020 the Finnish National Seismic Network (network code HE) consists of 31 permanent
49 seismic stations, including the FINES array. Nine stations are part of the Northern Finland
50 Seismic Network (FN) maintained by the Sodankylä Geophysical Observatory, University of
51 Oulu (Kozlovskaya et al., 2016). Data from these stations are integrated in the daily seismic
52 analysis and research at the National Seismological Data Center at ISUH. One station in the
53 Åland archipelago in southwestern Finland is operated by the Swedish National Seismic
54 Network. Figure 1 shows these stations on a map with earthquakes in Finland and adjacent areas.

55

56 Bilateral agreements allow for data exchange from stations close to the Finnish border collected
57 by seismological agencies in the neighboring countries Sweden, Norway, Estonia and Russia.

58 These data reduce the azimuthal gaps and thus improve the detection and location of the seismic
59 events that occur in Finland. In southern Finland, data from the Estonian network (EE) and in

60 northern Finland data from the Norwegian (NS, NO) and Swedish (UP) networks are frequently
61 used. EE is operated by the Tallinn University of Technology, NS by University of Bergen, NO

62 by NORSAR, and UP by Uppsala University. To the east of Finland, data from GEOFON

63 Seismic network (GE) station PUL, and Ida Network (II) station LVZ are used. Figure 2a shows

64 the azimuthal gap over the region when only the permanent Finnish stations are taken into

65 account. Figure 2b shows the azimuthal gap for the improved situation where all permanent

66 stations with constant data exchange are considered. Part of data are routinely transferred to the

67 GEOFON waveform archive hosted by GFZ German Research Centre for Geosciences and

68 ORFEUS. All seismic stations in the HE network are equipped with broadband seismometers.

69 The sensor instrumentation comes from manufacturers Geotech, Guralp, Nanometrics, and
70 Streckeisen, while the accompanying digitizers are from Earthdata, and Nanometrics.
71
72 Finland is situated on the Fennoscandian Shield, where the surface area covers some of the most
73 ancient crust of Earth from Precambrian time (Lehtinen et al., 2005). Most seismic stations have
74 been deployed on bedrock outcrops, and some FN stations such as OLKF (66.321° N, 29.400° E;
75 see Figure 1) have been installed in boreholes drilled into the bedrock. The seismic waveform
76 data are of high quality, not only due to state-of-art instrumentation, but also due to the
77 crystalline bedrock and only thin sedimentary layer where it exists (Nironen, 2017; Tiira et al.,
78 2020). In contrast, the geology of Estonia, our southern neighbor, is characterized by a
79 sedimentary layer hundreds of meters thick that increases towards the south (Raukas and
80 Teedumäe, 1997).
81
82 Data from all seismic stations fuel research activities, including investigations of postglacial
83 faults, shallow swarm-type seismicity, and properties of induced seismicity. Temporary local
84 seismic networks have been installed for research purposes in the Kuusamo and Kouvola
85 regions, which exhibit a higher level of natural seismicity compared to other parts of the country
86 (Veikkolainen et al., 2017). In addition, a local network of eight stations has been installed to
87 monitor the site of a possible future nuclear power plant in Ostrobothnia, according to
88 regulations of the International Atomic Energy Agency (Vuorinen et al., 2019). Data from the
89 Ostrobothnian deployment have been important for developing a ground-motion prediction
90 equation for Fennoscandia (Fülöp et al., 2020). The areas of notable seismic interest as well as
91 earthquakes of $M_L 0.0$ and greater are plotted in Figure 1, along with permanent seismic stations

92 in Finland. Probability density functions of power spectral density (PSD PDFs; McNamara and
93 Buland, 2004) for selected stations show low ambient noise. They are available in Figures S1-S4
94 in the electronic supplement to this article.

95

96 The use of carbon-neutral sources of energy is on the increase in Finland, and geothermal energy
97 is considered to have a lot of potential. A consequence is a new focus on urban areas which were
98 previously disregarded in seismic monitoring. A semi-permanent network of five seismic
99 instruments was deployed around the site of a geothermal heating facility in Espoo in the
100 Helsinki capital region to monitor induced earthquakes and to regulate operation during the
101 stimulations in 2018 and 2020 (Ader et al., 2020). The network was complemented by the
102 temporary deployment of dozens of short period sensors arranged in different array
103 configurations (Hillers et al., 2020). Data from the temporary networks used in such projects
104 may have restricted data access (Hillers et al., 2019).

105

106 Another network consisting of three stations with the same instrumentation as the national
107 network has been established in Helsinki following the initiative of the City of Helsinki. Data
108 from the Helsinki network follow the same standards as the national network. The Helsinki
109 network allows for monitoring seismicity in the Helsinki region with lower detection threshold
110 and better location accuracy than before and is expected to facilitate research on natural and
111 induced seismicity as well as on the numerous explosions associated with infrastructure
112 development in urban areas.

113

114 **Automatic Seismic Data Classification and Magnitude Determination**

115

116 In a seismically quiet intraplate region, most seismic events are explosions. Since May 2010,
117 only local events have been processed in the daily analysis of the FNSN, except for events from
118 known nuclear test sites. Events at a distance larger than 1000 km from Oulu, Finland (65.017°
119 N, 25.467° E; see Figure 1) are regarded as teleseismic events which are not processed in the
120 daily analysis. Oulu has been selected as the reference location because it is located very close to
121 the geographic center of the analysis area.

122

123 Until May 2010, teleseismic events were routinely reviewed. As real time data access and
124 seismic data analyses methods have developed, hand picking data in national data centers was no
125 longer needed for global seismic research. Shift on focus of analyses to local seismology had
126 become possible as the instruments got better, and station network denser, providing data on
127 higher frequencies and sufficient network coverage to detect and analyze typically small local
128 events. Detection of large global earthquakes is still implemented in the national natural disaster
129 warning system LUOVA maintained by ISUH in co-operation with the Finnish Meteorological
130 Institute and the Finnish Environment Institute (Säntti and Kortström, 2010) under the control of
131 the Finnish Ministry of Transport and Communications. No routine analysis of waveform data is
132 carried out in the on-duty LUOVA service except for nuclear tests for which data from the
133 FINES array are used. Waveform data from the FINES array are continuously transferred to the
134 headquarters of the CTBTO using a secured satellite network.

135

136 The automatic seismic event classification tool Automaija (Kortström et al., 2016) uses the
137 signal energy distribution of the incoming waveform data to detect seismic events and to

138 distinguish between natural and anthropogenic events. It calculates a preliminary origin time,
139 location and magnitude for each event. It also analyzes the probability for each event to be an
140 earthquake or explosion, and provides timing for identifiable seismic phases. Automaija
141 classifies seismic data to seven different groups:

142

- 143 1. probable earthquakes
- 144 2. uncertain classification
- 145 3. no recognizable station (this previously included events only observed by FINES;
146 this is a legacy category to be removed in future)
- 147 4. no classification, small or only observed by FINES
- 148 5. probable explosion
- 149 6. possible explosion at a mining site
- 150 7. probable explosion located at a mining site

151

152 For groups 6 and 7, the system relies on an internal database of mining sites in the analysis
153 region. A separate flag is given for events for which the closest operating seismic station is any
154 of the Ostrobothnia network stations. The success rate of Automaija classifications is 94-97% for
155 all data, as determined subsequently by comparing reviewed daily analysis results with automatic
156 determinations. The rate is slightly better for events with higher magnitudes and larger depths.
157 The daily and weekly distribution of events is utilized to resolve a blasting time window for each
158 mine, and signals not associated with natural earthquakes within this time-space window are
159 interpreted as recurring blasts. Successive explosions with a very small time interval so that
160 signals overlap may be sometimes mistaken for earthquakes in the fully automatic classification

161 process, due to misidentification of phases after the first P- and S-wave picks. For shallow events
162 with assigned fixed depths, more accurate location and depth estimates may be obtained by
163 studying the maximum amplitude ratio of Rayleigh wave R_g to S_g as done e.g. for swarm-type
164 seismicity in the relatively homogeneous Vyborg rapakivi granite batholith (Uski et al., 2006) in
165 the southeast of Finland.

166

167 Calculation of distance and back azimuth to the epicenter is based on travel time differences of
168 seismic phases and on the ISUH crustal model. For Finnish earthquakes, the automatic procedure
169 usually estimates location, time and magnitude from waveform data better than depth, and
170 therefore in automatic processing, the depth is always fixed to zero. In manual analyses the depth
171 is fixed if the standard deviation of depth determinations of permanent stations is more than 30%
172 of the estimated depth value, if the distance to the closest station is larger than 100 km, or the
173 azimuthal gap is greater than 180° . The typically used values for fixed depths are 1, 2, 5, 10 and
174 15 km. In particular, shallow events with clearly discernible surface waves often fall into this
175 category. Although FNSN is a relatively sparse network, the locations of its stations have been
176 optimized to keep the azimuthal gap below 90° over most of the territory. The situation is
177 poorest in eastern Finland (Figure 2), and data from seismic stations in northwestern Russia do
178 not improve the situation significantly. Although the number of seismic stations in this region is
179 reasonable (Morozov et al., 2019), only the PUL and LVZ stations occasionally provide
180 waveform data for our analysis.

181

182 All FNSN seismic stations deliver waveform data in vertical, east/west and north/south
183 components. The magnitude used is the local Helsinki magnitude $M_L(\text{HEL})$ (Uski and

184 Tuppurainen, 1996), which is always calculated from the vertical component. The magnitude
185 was originally estimated using the period and arrival time of Sg phases recorded at stations with
186 distances greater than 150 km from the epicenter, but the method has been further developed so
187 that it is valid also for shorter distances.

188

189 When $M_L(HEL)$ was introduced in the late 1990s, instruments were mainly short-period,
190 operating with a comparatively low sampling rate of 20 Hz. Very sparse near-source data are
191 available from this time. Modern broadband seismometers with a sampling rate of 40-500 Hz
192 have been deployed since then, and the station density of the network increased in tandem,
193 leading to more accurate magnitude estimates.

194

195 All individual FNSN stations transmit continuous waveform data to the ISUH servers at a
196 sampling frequency of 100-250 Hz, and all FINES array substations at a frequency of 40 Hz.
197 Data are stored in miniSEED archive format, with event files stored separately in CSS 3.0 format
198 (Anderson et al., 1990). These are further processed using the Geotool software (Henson and
199 Coyne, 1993) in the daily analysis. Seismogram data are produced for visual inspection in three
200 time intervals: 0-8, 8-16 and 16-24 UTC (local time is in the East European Standard Time Zone
201 EEST, UTC+2). These data are updated hourly. The amplitude of the ambient noise in the data
202 typically varies with the atmospheric and weather conditions. Most permanent stations are
203 situated in wind-shielded cabins outside major population centers and away from large water
204 bodies. However, an adequate network geometry means that certain stations are inevitably
205 located close to the Baltic Sea. The detection threshold of the network is $M_L0.9$ for the Finnish
206 territory as determined with seismic network simulations, using magnitude and maximum

207 detection distance (Tiira et al., 2016). The threshold is significantly lower in areas with network
208 densifications.

209

210 In the current ISUH crustal velocity model, the topmost granitic layer spans from surface to 15
211 km depth, and the basaltic layer from 15 km to 40 km, which is the Moho depth. P-waves and S-
212 waves refracted from the granitic layer are indicated with g (Pg, Sg), waves refracted from
213 basaltic layer with b (Pb, Sb), and waves refracted from the Moho with n (Pn, Sn). A three-
214 dimensional crustal velocity model is being developed at ISUH and will be implemented in the
215 daily workflow of event determination. The model utilizes results of numerous Finnish structural
216 seismology experiments and tomographic studies (e.g. Tiira et al., 2020; Hyvönen et al., 2007;
217 Kukkonen and Lahtinen, 2006). It is expected to be a significant improvement over the current
218 layer-cake model for providing more accurate location estimates.

219

220 In 2018 (2019), the FNSN stations detected 19431 (20286) seismic events, of which 421 (371) or
221 2% (2%), were interpreted as earthquakes. The overwhelming number of seismic events not
222 classified as earthquakes are explosions, mining-induced events or unidentified events in the
223 classification scheme used by the institute. The increase of detected events from 2018 to 2019 is
224 most likely a result of an improved network which can more easily detect anthropogenic seismic
225 sources especially in the Finnish capital region. The decrease of the seismic background noise
226 during the societal restrictions of Covid-19 pandemic was also visible in Helsinki and its
227 vicinity, in line with global trends (Lecocq et al., 2020), albeit in a higher frequency band.

228

229 **NorDB Database and NorLyst Analysis Tool**

230

231 Since 2017, the NorDB database has been developed at ISUH to store Nordic format seismic
232 data in a secure and coherent manner. The database runs on PostgreSQL and Python 3 in Unix-
233 based operating systems. It is currently only used internally at ISUH, although it can handle all
234 Nordic format data from other countries as well. NorDB is accessible via command line tool,
235 through which most basic functions are available. The Nordic event table is the most important
236 item in the database, linking one seismological event to all relevant metadata. The Nordic event
237 table also links to a Nordic event root table, which links to all different analyses of the same
238 event. These analyses can include the automatic solution and various analyst-reviewed solutions.
239 This technique ensures that there is no need to delete old records of the event when a new
240 analysis is completed. In addition, all analyses can adhere to a strict hierarchy by comparing their
241 event type.

242

243 In the NorDB structure, each seismic event is read from a file contained in a Nordic filename
244 table. New events from the network are automatically fed to the database using a shell script
245 which generates a date and timestamp to a creation information table. Because the script is
246 usually run periodically, creation information may be the same for various events with different
247 origin time. Instrumental data related to each event includes information about the number of
248 observing stations, azimuthal gap and minimum distance to a station for all data from year 2000
249 and younger.

250

251 Each solution of a seismic event in NorDB is associated with a permanent unique identifier. The
252 same event may have two or more solutions in the database with different solution types. The
253 currently used values of solution type are:

254

- 255 • F (final)
- 256 • A (automatic)
- 257 • O (other)
- 258 • REV (reviewed event)
- 259 • TRASH (duplicates as well as noise and incorrect data)

260

261 Automatic events (A) are pushed to the database each night, and reviewed in the daily analysis.
262 After the analysis of an event, a reviewed solution (REV) is generated but the automatic solution
263 for the same event is still retained in the database. Final event solutions (F) are generated when
264 seismic bulletins are constructed, but the two other solutions (A) and (REV) are retained also in
265 this situation. The user may also add new solution types to the database. In addition to solution
266 types, solution tags may be added to the database in the future. Tags are intended for
267 distinguishing project data from other data.

268

269 The seismic analysis tool NorLyst fetches data from NorDB. It features a graphical user interface
270 based on PyQt5 (Figures 3 and 4), allowing the user to filter seismograms, view spectra and
271 carry out other core analysis tasks.

272

273 The focus of analysis is nowadays on the verification of automatically detected events rather than
274 picking events manually. Fully manual analysis is conducted for earthquakes and exceptionally
275 large or otherwise interesting societally relevant seismic events, such as mine collapses or events
276 that could be induced by other engineering activity. In June 2020, the analysts of the institute
277 began using NorLyst for reviewing events which do not require manual picking of seismic
278 phases. Most of these are explosions from mines in Finland and adjacent areas. Geotool is still
279 used for manual picking of seismic phases, and manually analyzed Nordic files are typically
280 imported to NorLyst before the completion of the daily analysis in NorLyst.

281
282 The stable version of NorDB runs on a database server at ISUH and automatic backups are
283 generated to a server in aremote location once a day. Development of the database continues, and
284 the data structure, which now closely follows the Nordic format, may be updated in the future.
285 For example, the need for calculating more than three magnitudes for a certain event will be
286 considered. Other development targets include the removal of the need for reconfiguring NorDB
287 for a certain user after installing a version update, and the direct transfer of macroseismic data to
288 the database.

289

290 **Macroseismic Observatory Practice in Finland**

291
292 Macroseismology is an important interface between the seismological community and the
293 general public. The crystalline bedrock and low attenuation of seismic waves makes it possible
294 for the local population to observe and experience even low-magnitude seismic events. Since the
295 turn of the 2000s, an online macroseismic questionnaire is maintained on the ISUH website,

296 available in Finnish, Swedish and English. Submission of an observation automatically transfers
297 it to a spreadsheet file at the server. Seismologists and seismic analysts handle the data according
298 to the General Data Protection Regulation of the European Union. All personal information is
299 removed 30 days after the submission. Prior to this, the observer is contacted upon request.

300 Macroseismic intensity is not assigned to locations routinely because of the low magnitudes, but
301 the observations are classified into categories of ‘not felt’ and ‘felt’ and/or ‘heard’. Larger-
302 magnitude earthquakes can be subjected to specific macroseismic investigations. In the ISUH
303 seismic bulletins, the code ‘FELT’ is used for events observed by citizens.

304

305 The online macroseismic data are strongly biased towards positive responses, but they are
306 obtained without any survey launched by seismologists. Combined with the denser networks
307 available today this means that macroseismic observations can be associated with very small
308 events, far below M_L1 , if they are shallow, and close to population centers. Seismic events
309 observed non-instrumentally in the 2000s include local, regional and global earthquakes, induced
310 earthquakes, explosions, cryoseisms, and supersonic booms. Providing an accurate reason for the
311 observation has value in situations of sudden confusion and concern by citizens.

312

313 In 2019 ISUH received 496 macroseismic observations, 98 of which could be associated with a
314 known earthquake. Other sources were supersonic booms (19 observations), a sewage plant
315 construction site (30) and quarry explosions (75). For 251 observations, no specific source could
316 be identified.

317

318 The second important reason behind continued macroseismic activities is comparison with pre-
319 instrumental earthquakes. The seismicity record can be extended back in time about three
320 centuries with the help of pre-instrumental data (Mäntyniemi 2017a,b). The time span is
321 sufficient to demonstrate that earthquakes with larger areas of perceptibility have occurred in the
322 past, although they have not occurred during the instrumental era. The Lurøy, Norway,
323 earthquake of 31 August 1819 is an illustrative example (Mäntyniemi et al., 2020).

324

325 **The 2017 M_L3.3 Liminka earthquake - an Example of Collecting Waveform** 326 **and Macroseismic Data**

327

328 Waveform data from all permanent seismic stations in Finland can be conveniently processed
329 using ObsPy modules of the Python language (Krischer et al., 2015). Here we present an
330 example of handling waveform data from one of the deepest earthquakes in Finland. It occurred
331 in Liminka, northern Ostrobothnia, on 7 December 2017 at 22:32:16.6 UTC (8 December at
332 00:32:16.6 local time), and was assigned a local magnitude of 3.3. It was the strongest
333 earthquake in Finland since the M_L3.5 Kuusamo event of 15 September 2000. The Liminka
334 event was located at 64.785° N, 25.370° E, at the boundary of mudstone-dominated lithology in
335 the north and granitoid-dominated lithology in the south. This is 25 km north-northeast of
336 downtown Oulu and 10 km south-southwest of the nearest known surface fault, yet the true
337 distance to this fault may differ because the event was as deep as 32 km as estimated from data
338 of OBF0-OBF8 stations (Vuorinen et al., 2018). See Figures 5 and 6 for details.

339

340 As part of the annual reporting of operation and seismic activity in the area monitored by OBF0-
341 OBF8 stations, a fault plane solution is available for the earthquake. The solution shows a mainly
342 horizontal dislocation along the strike of the fault. The fault plane is nearly vertical and in north-
343 northwest - south-southeast direction (strike 333° , dip 87° , rake -20°). The auxiliary plane (strike
344 65° , dip 70° , rake 176°) is an unlikely solution considering the local geology. Some uncertainty
345 in the solution is evident because the event was located outside the local network, yet the
346 solution is very similar to solutions for other smaller earthquakes in the same region and is
347 therefore assumed to reflect the general trend of tectonic structures in the area. The similarity to
348 the fault plane of the $M_L 1.3$ earthquake in Lumijoki on October 8, 2018, is particularly important
349 because the epicentral distance between these two events is only 14 km (Vuorinen et al., 2018).
350 It is possible that the events occurred on the same fault, particularly because the Lumijoki event
351 also was deep, with a focal depth of 28 km. The azimuth, as seen from the Liminka event, also
352 follows the trend of faults in the area. The fault plane of the Lumijoki earthquake strongly
353 resembles that of Liminka event (strike 329° , dip 78° , rake -9°) and of the auxiliary plane (strike
354 61° , dip 81° , rake -168°).
355
356 ISUH received over 500 citizen observations of the Liminka earthquake. These are illustrated in
357 Figure 5. The farthest observations were over 240 km from the epicenter. In the vicinity, ground
358 shaking was widely felt (intensities IV, IV-V, V EMS-98), but no damage to property was
359 reported. Instrumental data were available from stations at much longer distances. Figure 6
360 shows waveform data of the Liminka earthquake recorded by the Oulainen (OUF) and
361 Kuusamo/Riekkii (KU6) stations located 56 km and 251 km from the epicenter, respectively. The
362 event was also observed by all OBF stations (Valtonen et al., 2013) that were all located less

363 than 100 km away from the epicenter with an azimuth range of 187°-284° (south to west-
364 northwest). The azimuthal gap of the event was only 49° and reliable observations were available
365 from as many as 42 stations, the farthest ones being in Åland (AAL) and Kevo (KEV), at 584 km
366 and 560 km distance. This is an exceptionally large number of stations that contributed to the
367 observation of an earthquake in Finland.

368

369 **Finnish Waveform Data and Online Services in EPOS**

370

371 Integration of ISUH services to European Plate Observing System (EPOS) is in progress in the
372 framework of the FIN-EPOS (The Finnish Initiative for EPOS) consortium (Korja and Vuorinen,
373 2016). FIN-EPOS is a consortium of Finnish universities (University of Helsinki, University of
374 Oulu, Aalto University) and research institutions (Geological Survey of Finland, National Land
375 Survey, Finnish Meteorological Institute, VTT Technical Research Centre of Finland, CSC - IT
376 Centre for Science) with the core task of maintaining geophysical observatories and laboratories
377 in Finland. In addition to the University of Helsinki, the Sodankylä Geophysical Observatory at
378 the University of Oulu produces and delivers seismic data and services in the FIN-EPOS
379 framework.

380

381 EPOS is the pan-European research infrastructure for data in Solid Earth Geophysics, aiming to
382 support a safe and sustainable society. In the Nordic countries, its implementation in the form of
383 Nordic EPOS has been initiated recently, but the history of Nordic co-operation in seismology
384 dates further back. The Nordic Seminars in Seismology have been organized since 1969 in
385 Finland, Sweden, Norway, Denmark and Iceland to provide an annual forum for interaction and

386 exchange, and Nordic format has been applied for seismic bulletin data since 1985 to allow
387 convenient data transfer. However, QuakeML is the standard seismological data format within
388 EPOS. Tools for data conversion between Nordic and QuakeML formats have been developed at
389 the University of Bergen, Norway (Rønnevik et al., 2019). Using NorDB, the conversion
390 between Nordic files and QuakeML is also possible.

391
392 ISUH offers an online map search tool to locate earthquakes from the North European Seismic
393 Catalogue (FENCAT; Ahjos and Uski, 1991). The catalogue includes natural seismic events only
394 and therefore excludes induced earthquakes. In the map and search results, all reviewed data
395 from ISUH seismic bulletins are included. Bulletin data marked “preliminary” at the website
396 have undergone the daily analysis workflow and can be used in research, but are potentially
397 subject to small updates related to magnitude homogenization, and addition of data from partner
398 institutions. No waveform data are provided via this service, but future plans include a browser-
399 based interface of NorLyst for review of seismic event locations without the need to install
400 software locally. We also aim at the integration of the online earthquake map to NorDB.

401

402 **Data and Resources**

403

404 See <https://doi.org/10.14470/UR044600> for the description of Finnish National Seismic
405 Network, <https://geofon.gfz-potsdam.de> for GFZ German Research Centre for Geosciences and
406 <https://www.orfeus-eu.org> for ORFEUS. Reviewed FNSN seismic bulletin data obtained from
407 the daily analysis are accessible via <https://www.seismo.helsinki.fi/bulletin/list/norBull.html>.
408 Final bulletins after magnitude homogenization and addition of data from partner institutes are

409 available from 1991 to June 2018 and preliminary bulletins from July 2018 to recent days. Some
410 figures in this paper were generated using Generic Mapping Tools (Wessel et al., 2013), and
411 ObsPy (Krischer et al., 2015). The documentation of NorDB is available at
412 <https://nordb.readthedocs.io>, and is subject to changes during the development of the software.
413 Noise levels of seismic stations RMF, PVF, SUF, and VRF were investigated using PQLX
414 software (<https://ds.iris.edu/ds/nodes/dmc/software/downloads/pqlx>), and resulting PSD PDFs
415 for the period of January 1 to December 1, 2020 are provided in the form of electronic
416 supplement (Figures S1-S4). All links were last accessed on December 11, 2020.

417

418 **Acknowledgments**

419

420 We thank all contributing to the operation, maintenance and expansion of seismic networks in
421 Finland, and the Academy of Finland (FIN-EPOS), Finnish Ministry for Foreign Affairs, the City
422 of Helsinki, and Fennovoima Inc. for funding. The helpful comments and suggestions by Editor
423 in Chief Allison Bent, reviewer Emily Wolin and an anonymous reviewer were of great value.

424

425 **References**

426

427 Ader, T., M. Chendorain, M. Free, M., T. Saarno, P. Heikkinen, P. E. Malin, P. Leary, G.
428 Kwiatek, G. Dresen, F. Bluemle and T. Vuorinen (2020). Design and implementation of a traffic
429 light system for deep geothermal well stimulation in Finland, *J. Seismol.* **24** 991-1014.

430

431 Ahjos, T., and M. Uski, 1992. Earthquakes in northern Europe in 1375–1989, *Tectonophys.* **207**
432 1-23.

433

434 Anderson, J., W. E. Farrell, K. Garcia, J. Given, and H. Swanger (1990). *Center for Seismic*
435 *Studies Version 3 Database: Schema Reference Manual*, Center of Seismic Studies, Arlington,
436 Virginia, Technical Report C90-01, 61p.

437

438 Coyne, J., D. Bobrov, P. Bormann, E. Duran, P. Grenard, G. Haralabus, I. Kitov, and Y.
439 Starovoit (2012). CTBTO: Goals, Networks, Data Analysis and Data Availability, *in New*
440 *Manual of Seismological Observatory Practice 2 (NMSOP-2)* P. Bormann, (Editor), Deutsches
441 GeoForschungsZentrum GFZ, Potsdam, p. 1-41.

442

443 Fülöp, L., V. Jussila, R. Aapasuo, T. Vuorinen, and P. Mäntyniemi (2020). A ground-motion
444 prediction equation for Fennoscandian nuclear installations, *Bull. Seismol. Soc. Am.* **110** 1211-
445 1230.

446

447 Henson, I., and J. Coyne (1993). *The Geotool seismic analysis system*, Proceedings of the 15th
448 Annual Seismic Research Symposium, September 8-10, 1993, Phillips Laboratory report PL-TR-
449 93-2160.

450

451 Hillers, G., T. A. T. Vuorinen, E. J. Arola, V. E. Katajisto, M. P. Koskenniemi, B. M. McKeivitt,
452 S. Rezaei, L. A. Rinne, I. E. Salmenperä, P. J. Seipäjärvi, L. S. O. Väkevä, A. I. Voutilainen, K.
453 Arhe, A. K. Juntunen, J. Keskinen, P. Lindblom, K. Oinonen, and T. Tiira (2019). A 100 3-
454 component sensor deployment to monitor the 2018 EGS stimulation in Espoo/Helsinki, southern
455 Finland, Dataset. *GFZ Data Services*, doi:10.5880/GIPP.201802.1.

456

457 Hillers, G., T. A. T. Vuorinen, M. R. Uski, J. T. Kortström, P. B. Mäntyniemi, T. Tiira, P. E.
458 Malin, and T. Saarno (2020). The 2018 Geothermal Reservoir Stimulation in Espoo/Helsinki,
459 Southern Finland: Seismic Network Anatomy and Data Features, *Seismol. Res. Lett.* **91(2A)** 770-
460 786.

461

462 Hyvönen, T., T. Tiira, A. Korja, P. Heikkinen, E. Rautioaho, and SVEKALAPKO Seismic
463 Tomography Working Group (2007). A tomographic crustal velocity model of the central
464 Fennoscandian Shield, *Geophys. J. Int.* **168** 1210-1226.

465

466 Korja, A., and T. Vuorinen (2016). FIN-EPOS: Finnish national initiative of the European Plate
467 Observing System, in *Lithosphere 2016: Ninth Symposium on the Structure, Composition and*
468 *Evolution of the Lithosphere in Finland: Programme and Extended Abstracts* I. T. Kukkonen, S.
469 Heinonen, K. J. Oinonen, T. K. Arhe, O. Eklund, F. Karell, E. Kozlovskaya, A. V. Luttinen, R.
470 Lahtinen, J. Lunkka, V. Nykänen, M. Poutanen, E. Tanskanen, and T. Tiira (Editors), University
471 of Helsinki, p. 30-31.

472

473 Kortström, J., M. Uski, and T. Tiira (2016). Automatic classification of seismic events within a
474 regional seismograph network, *Comput. Geosci.* **87** 22-30.

475

476 Kozlovskaya, E., J. Narkilahti, J. Nevalainen, R. Hurskainen, and H. Silvennoinen (2016).
477 Seismic observations at the Sodankylä Geophysical Observatory: history, present, and the future.
478 *Geosci. Instrum. Meth.* **5** 365-382.

479

480 Krischer, L., T. Megies, R. Barsch, M. Beyreuther, T. Lecocq, C. Caudron, and J. Wassermann
481 (2015). ObsPy: a bridge for seismology into the scientific Python ecosystem, *Comput. Sci.*
482 *Discov.* **8** 014003.

483

484 Kukkonen, I.T., and R. Lahtinen (Ed.) (2006). *Finnish reflection experiment FIRE 2001–2005*,
485 Geological Survey of Finland, Special Paper 43, 247p.

486

487 Lecocq, T., S. P. Hicks, K. Van Noten, K. van Wijk, P. Koelemeijer, R. S. M. De Plaen, F.
488 Massin, G. Hillers, R. E. Anthony, M.-T. Apoloner, M. Arroyo-Solórzano, J. D. Assink, P.
489 Büyükakpınar, A. Cannata, F. Cannavo, S. Carrasco, C. Caudron, E. J. Chaves, D. G. Cornwell,
490 D. Craig, O. F. C. den Ouden, J. Diaz, S. Donner, C. P. Evangelidis, L. Evers, B. Fauville, G. A.
491 Fernandez, D. Giannopoulos, S. J. Gibbons, T. Girona, B. Grecu, M. Grunberg, G. Hetényi, A.
492 Horleston, A. Inza, J. C. E. Irving, M. Jamalreyhani, A. Kafka, M. R. Koymans, C. R. Labeledz, E.
493 Larose, N. J. Lindsey, M. McKinnon, T. Megies, M. S. Miller, W. Minarik, L. Moresi, V. H.

494 Márquez-Ramírez, M. Möllhoff, I. M. Nesbitt, S. Niyogi, J. Ojeda, A. Oth, S. Proud, J. Pulli, L.
495 Retailleau, A. E. Rintamäki, C. Satriano, M. K. Savage, S. ShaniKadmiel, R. Sleeman, E. Sokos,
496 K. Stammler, A. E. Stott, S. Subedi, M. B. Sørensen, T. Taira, M. Tapia, F. Turhan, B. van der
497 Pluijm, M. Vanstone, J. Vergne, T. A. T. Vuorinen, T. Warren, J. Wassermann, and H. Xiao
498 (2020). Global quieting of high-frequency seismic noise due to COVID-19 pandemic lockdown
499 measures, *Science*, doi:10.1126/science.abd2438.

500

501 Lehtinen, M., P. A. Nurmi, and O. T. Rämö (2005). *Precambrian Geology of Finland. Key to the*
502 *Evolution of the Fennoscandian Shield*, Developments in Precambrian Geology, Elsevier,
503 Amsterdam, 736p.

504

505 Luosto, U., and T. Hyvönen (2001). Seismology in Finland in the Twentieth Century,
506 *Geophysica* **37** 147-185.

507

508 McNamara, D. E., and R. P. Buland (2004). Ambient Noise Levels in the Continental United
509 States, *Bull. Seism. Soc. Am.* **94** 1517-1527.

510

511 Mäntyniemi, P. (2017a). Macroseismology in Finland from the 1730s to the 2000s. Part 1:
512 History of the Macroseismic Questionnaire, *Geophysica* **52** 3-21.

513

514 Mäntyniemi, P. (2017b). Macroseismology in Finland from the 1730s to the 2000s: Part 2: From
515 an Obligation of the Learned Elite to Citizen Science, *Geophysica* **52** 23-41.

516

517 Mäntyniemi, P. B., M. B. Sørensen, T. N. Tatevossian, R. E. Tatevossian, and B. Lund (2020). A
518 reappraisal of the Lurøy, Norway, earthquake of 31 August 1819, *Seismol. Res. Lett.* **91** 2462-
519 2472.

520

521 Morozov, A. N., N. V. Vaganova, Y. V. Konechnaya, I. A. Zueva, V. E. Asming, N. N.
522 Noskova, N. V. Sharov, V. A. Assinovskaya, N. M. Panas, and Z. A. Evtugina (2019). Recent
523 seismicity in northern European Russia, *J. Seismol.* **24** 37-53.

524

525 Nironen, M. (Ed.) (2017). *Bedrock of Finland at the scale 1:1 000 000 – Major stratigraphic*
526 *units, metamorphism and tectonic evolution*, Geological Survey of Finland, Special Paper 60,
527 128p.

528

529 Pirhonen, S. (1996). Seventy years of seismological recording in Finland, in *Seismograph*
530 *recording in Sweden, Norway, - with arctic regions, Denmark - with Greenland, and Finland R.*
531 Wahlström (Editor), Proceedings of the Uppsala Wiechert Jubilee Seminar, Uppsala University,
532 August 22-23, 1994, Uppsala, Sweden.

533

534 Raukas, A., Teedumäe, A. (1997). *Geology and Mineral Resources of Estonia*, Estonian
535 Academy Publishers, Tallinn, 436p.

536

537 Rønnevik, C., J. Havskov, T. Utheim, L. Ottemöller, K. Atakan, and J. Michalek (2019). Nordic
538 format (SEISAN) to QuakeML converter, *Geophys. Res. Abstr.* **EGU2019-15033**.

539

540 Sääntti, K., and J. Kortström (2010). Building the National Early Warning System for Natural
541 Disasters in Finland: LUOVA Project 2008-2010, in *The 41st Nordic Seminar on Detection*
542 *Seismology*, Aarhus, Denmark, p. 30-31.

543

544 Simojoki, H. (1978). *The history of geophysics in Finland 1828-1918*, Societas Scientiarum
545 Fennica, 157p.

546

547 Tiira, T., M. Uski, J. Kortström, O. Kaisko, and A. Korja (2016). Local seismic network for
548 monitoring of a potential nuclear power plant area, *J. Seismol.* **20** 397-417.

549

550 Tiira, T., T. Janik, T. Skrzynik, K. Komminaho, A. Heinonen, T. Veikkolainen, S. Väkevä, and
551 A. Korja (2020). Full-scale crustal interpretation of Kokkola-Kymi (KOKKY) seismic profile,
552 Fennoscandian Shield, *Pure Appl. Geophys.* **177** 3775-3795.

553

554 Uski, M., and A. Tuppurainen (1996). A new local magnitude scale for the Finnish seismic
555 network, *Tectonophys.* **261** 23-37.

556

557 Uski, M., T., Tiira, A. Korja, and S. Elo (2006). The 2003 earthquake swarm in Anjalankoski,
558 south-eastern Finland, *Tectonophys.* **422** 55-69.

559

560 Veikkolainen, T., I. T. Kukkonen, and T. Tiira (2017). Heat flow, seismic cut-off depth and
561 thermal modeling of the Fennoscandian Shield, *Geophys. J. Int.* **211** 1414-1427.

562

563 Vuorinen, T., O. Kaisko, J. Kortström, M. Uski, and T. Tiira (2018). *Operation and seismic*
564 *observations of seismic network OBF in 2017*, University of Helsinki, Institute of Seismology,
565 Report T-98, 38p. (in Finnish).

566

567 Vuorinen, T., P. Seipäjärvi, J. Kortström, M. Uski, and T. Tiira (2019). *Operation and seismic*
568 *observations of seismic network OBF in 2018*, University of Helsinki, Institute of Seismology,
569 Report T-99, 32p. (in Finnish).

570

571 Wessel, P., W. H. F. Smith, R. Scharroo, J. Luis, and F. Wobbe (2013). Generic Mapping Tools:
572 Improved Version Released, *EOS Trans. AGU* **94(45)** 409-410.

573

574 **Full mailing list for each author (all authors)**

575

576 Institute of Seismology, University of Helsinki, P.O. Box 68, 00014 University of Helsinki,

577 Finland

578

579 **List of Figure Captions**

580 **Figure 1.** Earthquakes (circle symbols, $M_L \geq 0$) in Finland and adjacent areas on a map with

581 Finnish seismic stations. Color and circle size scale with the magnitude of the event. Symbols are

582 slightly transparent, and for clarity, greater events are plotted with larger symbols. Areas of

583 notable seismic activity (Kouvola and Kuusamo) and those with network densifications (Helsinki

584 and Ostrobothnia) are labeled. Earthquake data derive from the FENCAT catalogue, covering

585 years 1375-2020.

586

587 **Figure 2 (a).** Map of permanent seismic stations in Finland. Stations of network densifications in

588 Ostrobothnia and Helsinki are excluded. Color scale shows the maximum azimuthal gap of a

589 seismic event recorded by these stations. Because data are transmitted to Finland from nearest

590 stations in neighboring countries as well, the true azimuthal gap in Finnish border regions is

591 smaller than that visible in the map. See Figure 2 (b) for a map with Finnish stations, and other

592 stations delivering data to ISUH. **(b).** Map of permanent seismic stations in Finland (triangles)

593 and adjacent areas (squares) delivering data to ISUH. Stations of network densifications in

594 Ostrobothnia and Helsinki are not shown. Color scale shows the maximum azimuthal gap of a

595 seismic event recorded by these stations. See Figure 2 (a) for a map with Finnish stations only.

596

597 **Figure 3.** Illustration of a daily event list in the user interface of NorLyst software. Events from
598 Monday, November 16, 2020 are shown here according to the classification scheme. Each event
599 class is associated with a specific color in the list and in the map.

600

601 **Figure 4.** Illustration of a confirmed earthquake from Raasepori, southern Finland on 16
602 November 2020 in the user interface of the Norlyst software. Waveform data and automatic
603 phase picks for stations that have registered the event are available by selecting events in the list.
604 Phase picks are denoted by green and red colors. In the event list, colors are the same as in
605 Figure 3. HEL1 and HEL5 are temporary stations in the Finnish capital region.

606

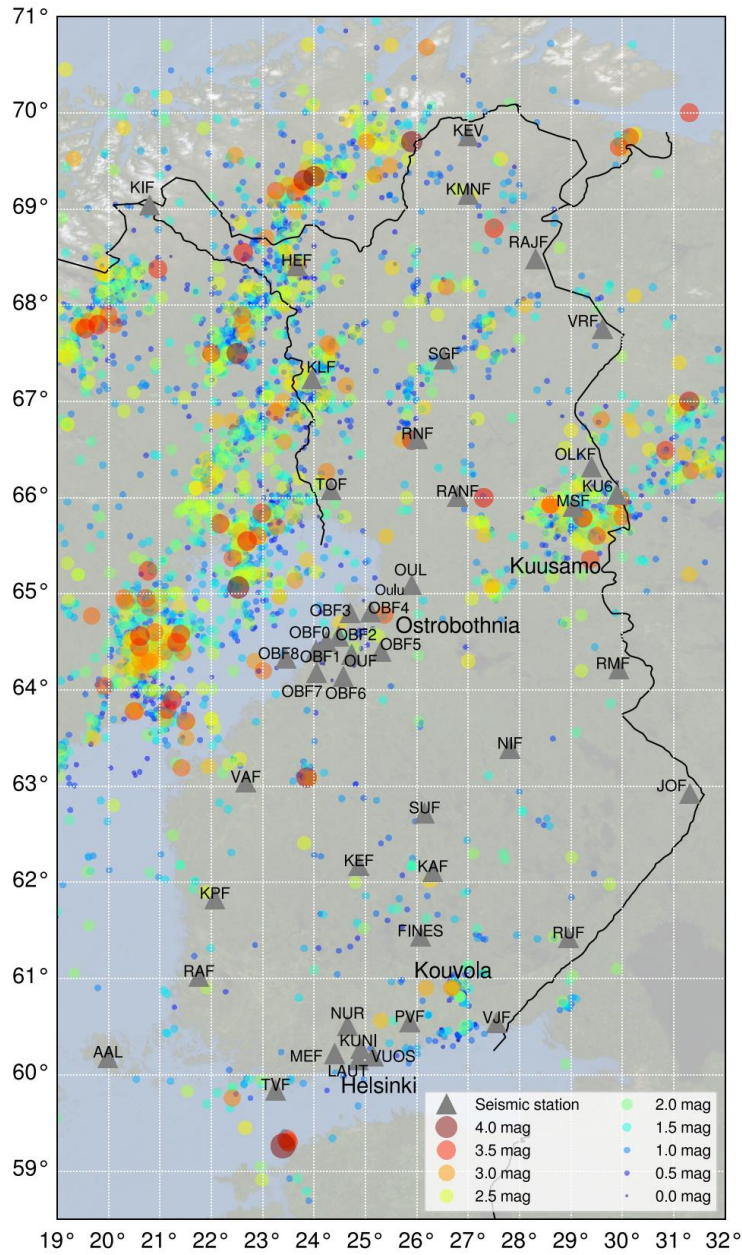
607 **Figure 5.** Macroseismic map of the $M_L3.3$ Liminka earthquake of 7 December 2017. The small
608 blue dots denote felt observations and the red dots audible ones. The shaded orange circular area
609 has a radius of 25 km around the epicenter, which is marked with a solid orange dot. Seismic
610 stations are denoted by triangle symbols. Locations of the city of Oulu, and other remarkable
611 towns are also shown.

612

613 **Figure 6.** Plotted waveform data of Liminka earthquake as observed by stations in Oulainen
614 (OUF) and Kuusamo/Riekki (KU6). Vertical axis shows the ground motion amplitude in
615 nanometers and horizontal axis the time in UTC.

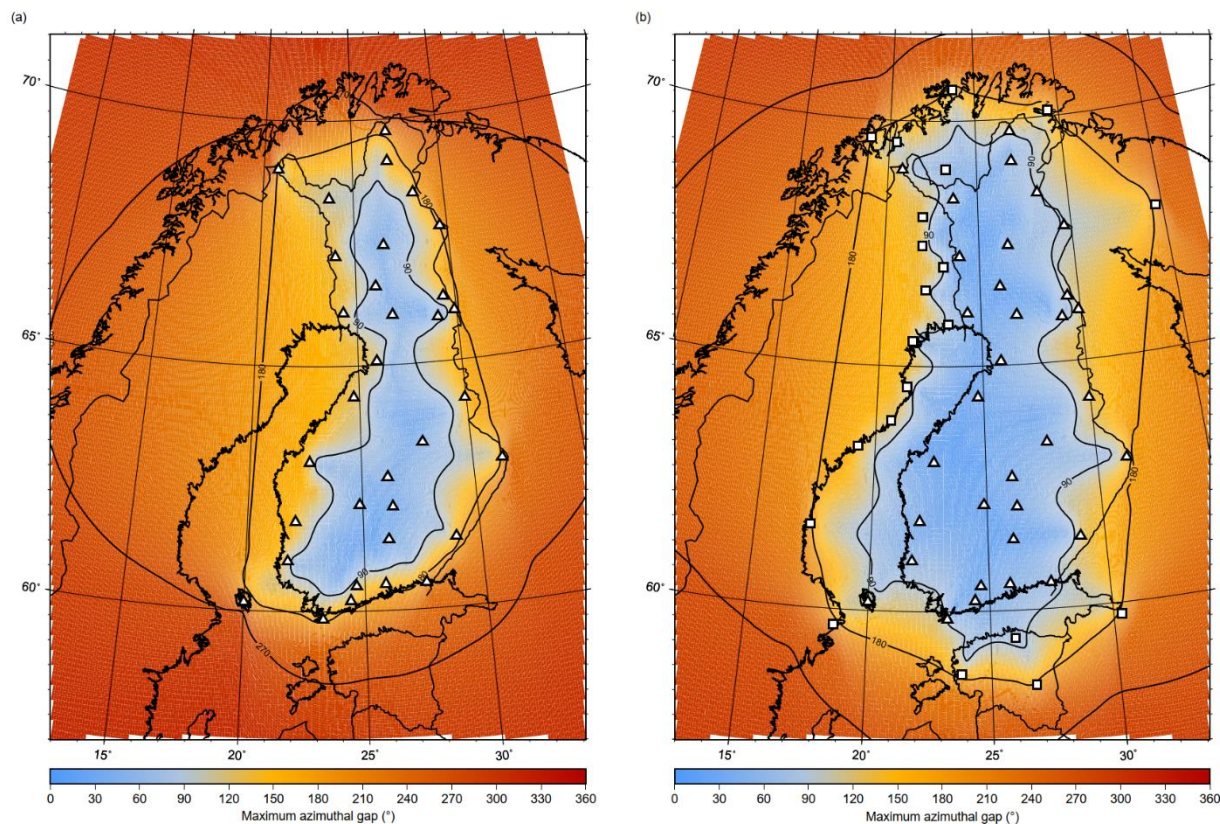
616

617 **Figures**

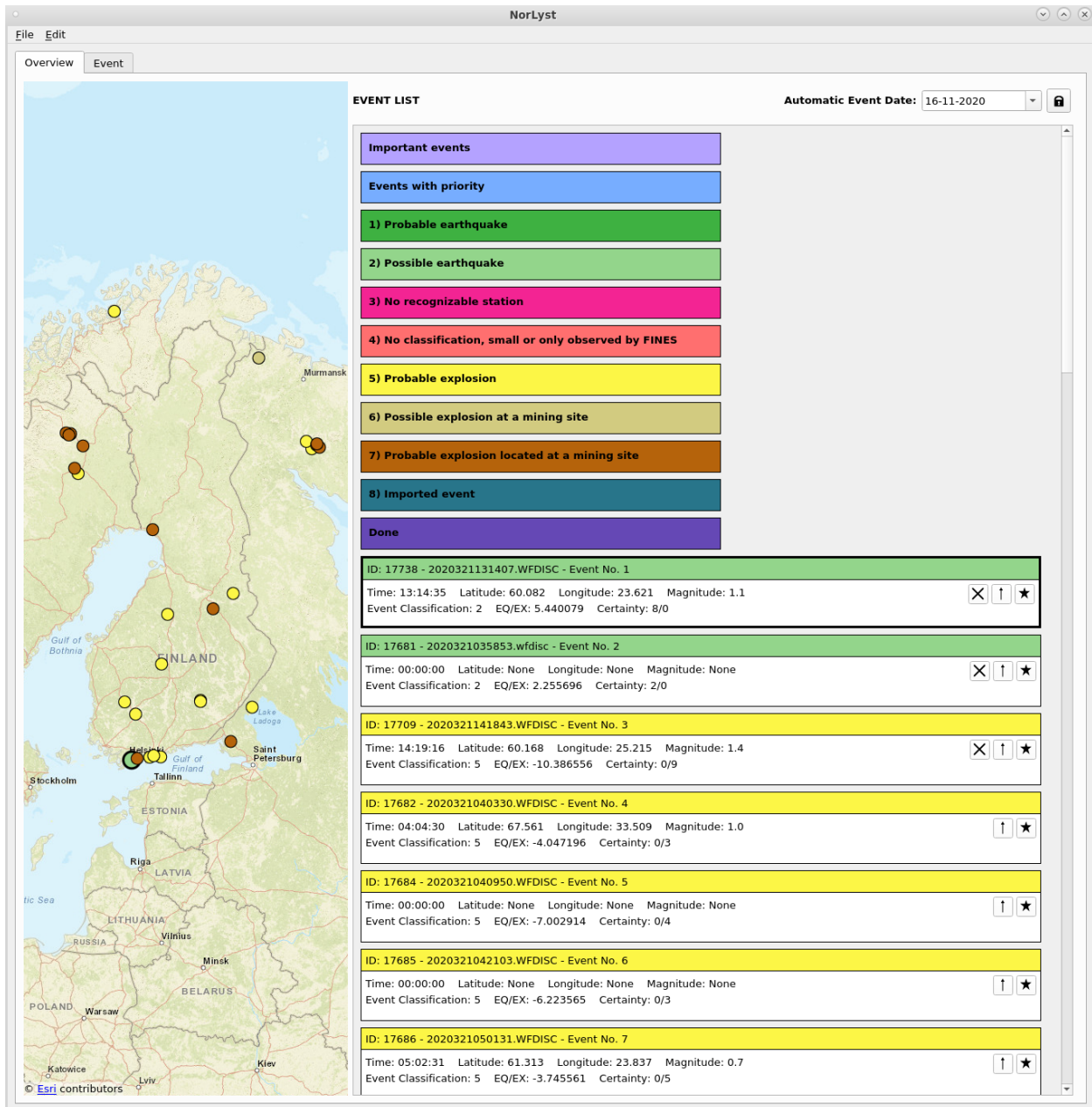


618

619 **Figure 1.** Earthquakes (circle symbols, $M_L \geq 0$) in Finland and adjacent areas on a map with
 620 Finnish seismic stations. Color and circle size scale with the magnitude of the event. Symbols are
 621 slightly transparent, and for clarity, greater events are plotted with larger symbols. Areas of
 622 notable seismic activity (Kouvola and Kuusamo) and those with network densifications (Helsinki
 623 and Ostrobothnia) are labeled. Earthquake data derive from the FENCAT catalogue, covering
 624 years 1375-2020.



625
 626 **Figure 2 (a).** Map of permanent seismic stations in Finland. Stations of network densifications in
 627 Ostrobothnia and Helsinki are excluded. Color scale shows the maximum azimuthal gap of a
 628 seismic event recorded by these stations. Because data are transmitted to Finland from nearest
 629 stations in neighboring countries as well, the true azimuthal gap in Finnish border regions is
 630 smaller than that visible in the map. See Figure 2 (b) for a map with Finnish stations, and other
 631 stations delivering data to ISUH. **(b).** Map of permanent seismic stations in Finland (triangles)
 632 and adjacent areas (squares) delivering data to ISUH. Stations of network densifications in
 633 Ostrobothnia and Helsinki are excluded. Color scale shows the maximum azimuthal gap of a
 634 seismic event recorded by these stations. See Figure 2 (a) for a map with Finnish stations only.
 635



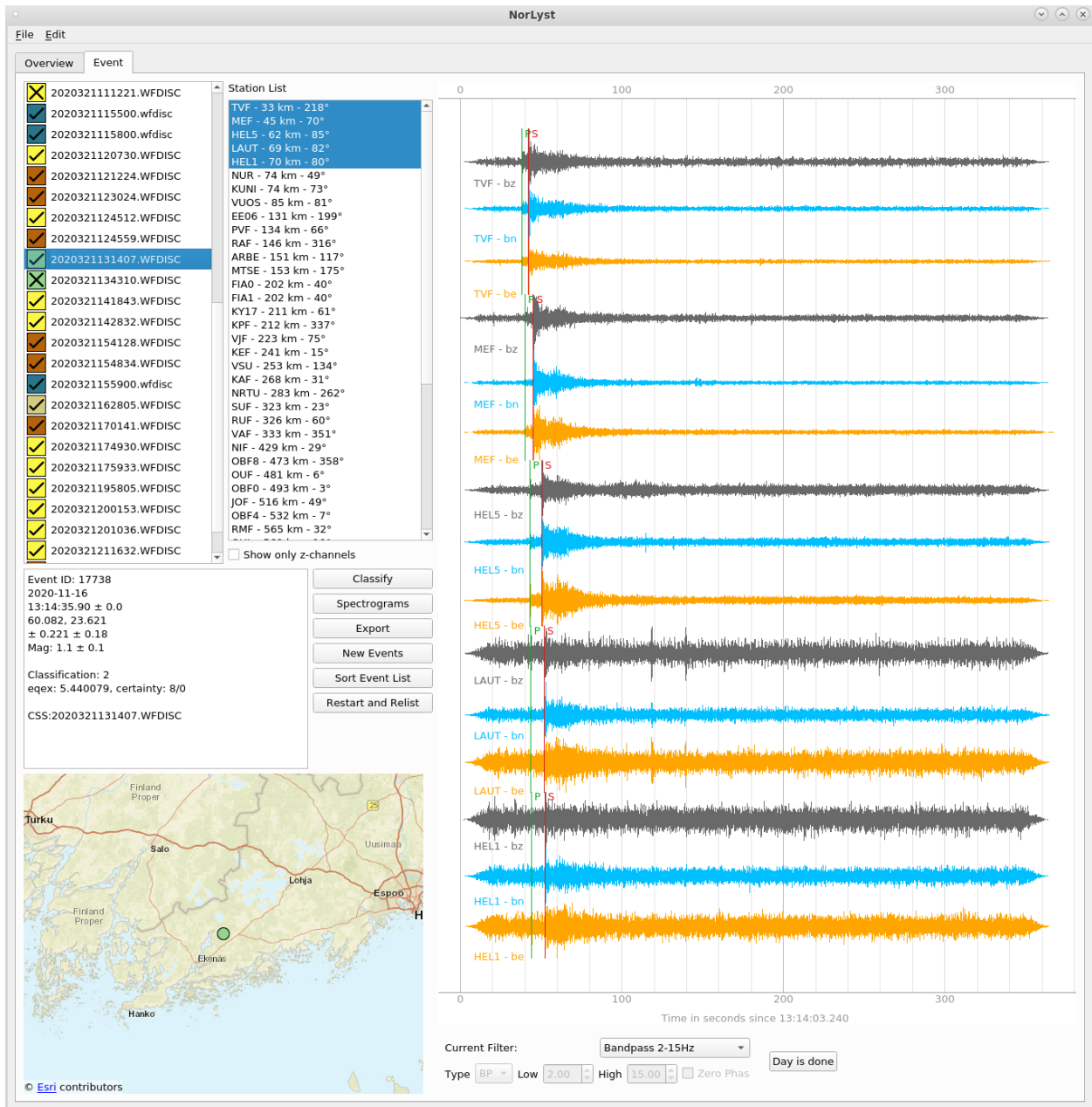
636

637 **Figure 3.** Illustration of a daily event list in the user interface of NorLyst software. Events from

638 Monday, November 16, 2020 are shown here according to the classification scheme. Each event

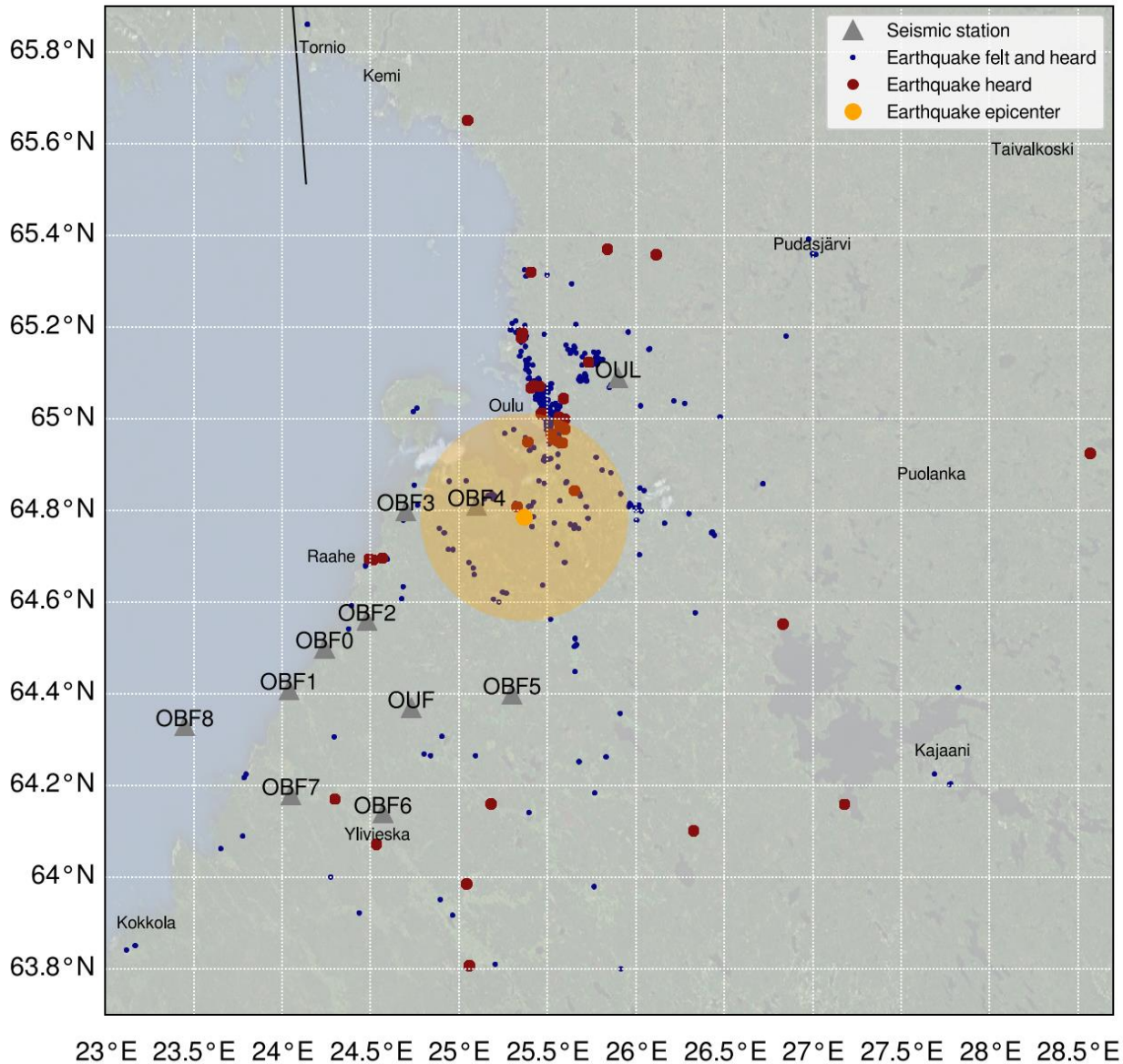
639 class is associated with a specific color in the list and in the map.

640



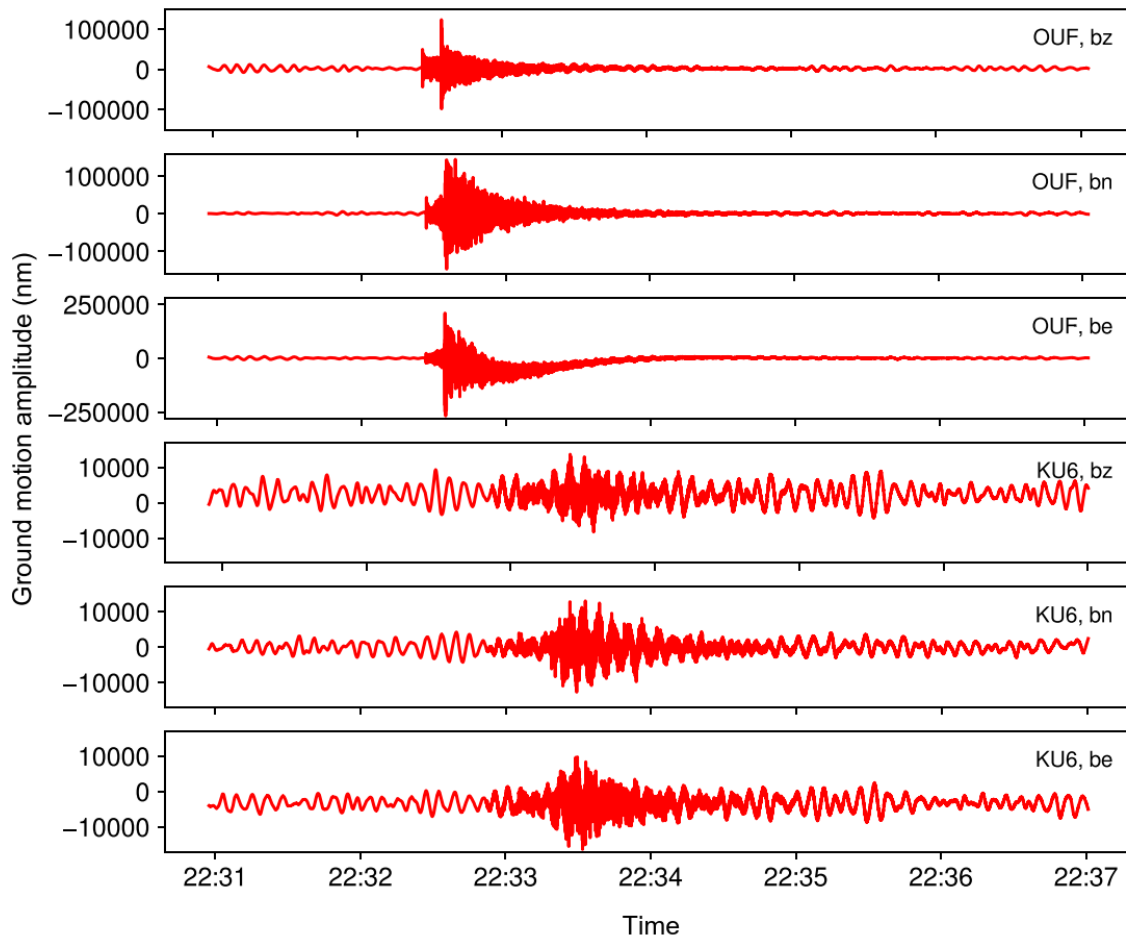
641
 642 **Figure 4.** Illustration of a confirmed earthquake from Raasepori, southern Finland on 16
 643 November 2020 in the user interface of the NorLyst software. Waveform data and automatic
 644 phase picks for stations that have registered the event are available by selecting events in the list.
 645 Phase picks are denoted by green and red colors. In the event list, colors are the same as in
 646 Figure 3. HEL1 and HEL5 are temporary stations in the Finnish capital region.

647



649 **Figure 5.** Macroseismic map of the M_L 3.3 Liminka earthquake of 7 December 2017. The small
 650 blue dots denote felt observations and the red dots audible ones. The shaded orange circular area
 651 has a radius of 25 km around the epicenter, which is marked with a solid orange dot. Seismic
 652 stations are denoted by triangle symbols. Locations of the city of Oulu, and other remarkable
 653 towns are also shown.

Liminka earthquake (M=3.3), Dec 7, 2017 at 22:32:16.6 (UTC)
observed by OUF and KU6 (at 56 km and 251 km distances)



654

655 **Figure 6.** Plotted waveform data of Liminka earthquake as observed by stations in Oulainen

656 (OUF) and Kuusamo/Rieikki (KU6). Vertical axis shows the ground motion amplitude in

657 nanometers and horizontal axis the time in UTC.